Independent component analysis approach to resolve the multi-source limitation of the nutating rising-sun reticle based optical trackers

Harold Szu [a], Ivica Kopriva [b,*], Antun Peršin [c]

[a] *Naval Surface Warfare Center, Dahlgren Laboratory, Dahlgren, VA 22448, USA*
[b] *Institute for Defense Studies, R&D, Bijenička 46, 10000 Zagreb, Croatia*
[c] *Institute ''Ruder Bošković'', Bijenička 54, 10000 Zagreb, Croatia*

Abstract

Independent component analysis (ICA) is described for a number of signals from different sources and a number of receivers. When applied to nutating rising-sun reticle optical trackers, ICA enables the discrimination of optical sources with an appropriate number of detectors. The main contribution of this paper is the conclusion that coherence between optical sources results in a nonlinear ICA problem that becomes linear when the optical fields are incoherent. It is shown that requirements necessary for the ICA theory to work are fulfilled for both coherent and incoherent optical sources. Moreover, it is shown additionally that by the proper design of the optical tracker the nonlinear model can be converted into linear one by simple linear bandpass filtering operation. Consequently, the multisource limitation of the nutating rising-sun reticle based optical trackers can in principle be overcome for both coherent and incoherent optical sources. © 2000 Elsevier Science B.V. All rights reserved.

1. Introduction

Reticle systems are considered to be the classical approach for estimating the position of a target in a considered field of view and are widely used in IR seekers [2]. The advantage of the reticle seekers is, because few detectors are used, simplicity and low cost [30,31]. Owing to a spatial filtering effect of the reticle, the IR reticle tracker may exclude unwanted background signals [2,3]. However, the major drawback of the reticle based trackers has been proven to be sensitivity on the IR countermeasures such as flares and jammers [4,30,31]. It has been shown in [1] that an optical system based on a nutating reticle can be modified to resolve the multisource limitation problem, [4], by the combined use of ICA theory and appropriate modification of the optical tracker design (see Fig. 3). Since reticle based optical systems are not a widely understood construct we present in

---

Section 2 a brief description of the optical modulation theory while more details can be found in [1–10]. It was assumed in [1] that the intensity of the incident optical field is the sum of single intensities that results in a linear convolutive signal model. We present in Section 3 a more rigorous statistical optics based derivation of the signal model [11,12]. It is shown that in the case of either partially or totally coherent optical fields the resulting signal model is nonlinear. When incoherence is assumed a linear model is obtained. Linear ICA is a very well understood subject and many algorithms are available to solve such problem [13–23]. The most distinguished approaches are based on the entropy maximization principle [13–15] and minimization of the fourth order cross-cumulants [23,24]. In [15] a unification of the unsupervised entropy maximization ICA and the energy minimization PCA. The nonlinear ICA is a more difficult problem, and only a few papers have addressed this subject for some special types of nonlinearity [13,25–28]. Therefore, it is shown at the end of Section 3 how, by the proper design of the optical tracking system, it can be ensured that nonlinear signal model be transformed into linear one by simple linear band-pass filtering operation. In Section 4 a brief discussion of the ICA theory requirements is given for linear and nonlinear signal models. Example of one adaptive ICA algorithm is briefly described in Section 5 while simulation results are presented in Section 6. Conclusions are given in Section 7.

2. Optical modulation theory

An optical system that uses either spinning or nutating reticle is used to detect and determine the
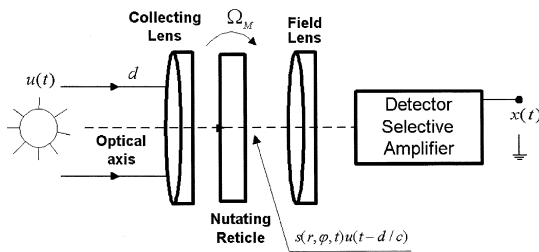
Fig. 1. Optical tracker.
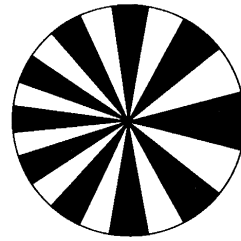
Fig. 2. Reticle with fan-bladed pattern.

position of an object from which some form of primarily IR energy is emitted, see Fig. 1, [1–10]. A moving reticle modulates the incidental optical flux and is located in the focal plane of an optical imaging system. Depending on the shape of the clear and the opaque segments, the optical flux after the reticle (i.e., on the output of the photodetector) is modulated in the appropriate way. Frequency modulation (FM) is used most often and is generated by nutating reticle with a fan-bladed pattern with clear and opaque segments (the rising-sun reticle), such as that shown in Fig. 2 or by the spinning reticles with different kind of the spokes geometry [5]. The deviation of the FM signal is directly proportional to the module of the polar coordinates (r, φ) of the optical source projection on the reticle area, while the phase of the FM signal is equivalent to the polar coordinate phase. It has been shown in [1] that instantaneous frequency of the source radiating flux after the reticle is given by

$$\hat{\omega}(t) = \omega_0 - \Delta\omega_m \cos(\Omega_M t - \varphi), \tag{1}$$

where

$$\omega_0 = n\Omega_M, \quad \Delta\omega_m = \Delta n\Omega_M. \tag{2}$$

and n is number of pairs of clear and opaque segments, Ω_M is the speed of nutation of the reticle and Δ is relative distance directly proportional to the module r. The time function with the instantaneous frequency that is based on Eq. (1) has the form

$$s(r, \varphi, t) = \cos[\omega_0 t - \beta \sin(\Omega_M t - \varphi)] \tag{3}$$

which is the canonical representation of an FM signal [29]. This waveform is actually the fundamental term of the photodetector response to the incident optical flux. The spectral terms around the frequencies $2\omega_0, 3\omega_0, \ldots$ exist, but the selective amplifier removes those terms [1,2,4]. Consequently, the inci-

dental optical flux at the detector area can be approximately described with $s(r,\varphi,t)u(t-d/c)$ where d/c represents time delay due to the time necessary for the optical field to propagate from the optical source to the detector.

3. Derivation of the signal model

We start with the problem of detecting optical radiation at point D when optical fields are emitted from two sources at points P_1 and P_2 (see Fig. 4). The optical field at point D is given as the sum of the individual fields multiplied by reticle modulating functions:

$$u_D(t) = K_1 u_1(t) s_1(t) + K_2 u_2(t-\Delta t) s_2(t) \qquad (4)$$

where Δt represents relative time delay between u_1 and u_2 due to the path length difference i.e. $\Delta t = (d_2 - d_1)/c$. In the case of the rising-sun reticle consisted of the clear and opaque segments, s_1 and s_2 are either 1 or 0 and are the functions of the coordinates of the optical source projections on the reticle area [1,2,4,5]. K_1 and K_2 are, in general, case complex constants representing path losses. We will assume here that they are real numbers. Detector will sense intensity obtained as [11,12]:

$$I_D(kT) = \langle u_D^*(t) u_D(t) \rangle \qquad (5)$$

where T represents detector averaging time and kT is new discretized time that allows treatment of nonstationarity. When (4) is applied to (5), I_D is obtained as:

$$I_D = I_1 s_1 + I_2 s_2 + 2 K_1 K_2 \sqrt{I_1 I_2} \, \text{Re}\{\gamma_{12}(\Delta t)\} s_1 s_2 \qquad (6)$$

In the expression (6) the time index is dropped in order to simplify notation. $\gamma_{12}(\Delta t)$ is the normalized mutual coherence function [11]:

$$\gamma_{12}(\Delta t) = \frac{\langle u_1(t) u_2^*(t-\Delta t) \rangle}{\sqrt{I_1 I_2}} \qquad (7)$$

Modulating functions s_1 and s_2 are functions of the coordinates of the corresponding optical sources only and are mutually independent. They are also independent relative to the optical fields u_1 and u_2. It is therefore possible to write:

$$K_1^2 \langle |u_1(t)|^2 s_1^2(t) \rangle = K_1^2 \langle |u_1(t)|^2 \rangle \langle s_1^2(t) \rangle = I_1 s_1,$$

since $s_1^2 = s_1$ and $\langle s_1 \rangle = s_1$ because the detector averaging process is fast in relation to the modulating function s_1. The same reasoning applies for s_2, which explains how the first two parts in expression (6) are obtained. The third part is obtained from:

$$2 K_1 K_2 \langle u_1(t) u_2^*(t-\Delta t) s_1(t) s_2(t) \rangle$$
$$= 2 K_1 K_2 \langle u_1(t) u_2^*(t-\Delta t) \rangle \langle s_1(t) \rangle \langle s_2(t) \rangle$$

because s_1 and s_2 are independent of u_1 and u_2 and also mutually independent. Taking into account (7) and $\langle s_1 \rangle = s_1$, $\langle s_2 \rangle = s_2$, the third part of expression (6) is obtained. The photocurrent is obtained when the intensity I_D is expressed in terms of spectral irradiance and when detector spectral responsivity is taken into consideration, giving:

$$i(kT) = A \int I_1(\lambda, kT) R(\lambda) d\lambda \times s_1(kT)$$
$$+ A \int I_2(\lambda, kT) R(\lambda) d\lambda \times s_2(kT) + 2 K_1 K_2$$
$$\times \sqrt{\int I_1(\lambda, kT) R(\lambda) d\lambda \times \int I_2(\lambda, kT) R(\lambda) d\lambda}$$
$$\times \text{Re}\{\gamma_{12}(\Delta t)\} \times s_1(kT) s_2(kT), \qquad (8)$$

where A is the detector sensing area and λ is wavelength. When in accordance with Fig. 3 the beam splitter and two detectors are used, Eq. (8) can be used to obtain expressions for the corresponding photocurrents by simply inserting $\tau(\lambda)$ and $\rho(\lambda)$ into integrals over λ in (8). Here $\tau(\lambda)$ and $\rho(\lambda)$ are beam splitter transmission and reflection coefficients, respectively. Responsivity $R(\lambda)$ should be replaced with $R_1(\lambda)$ when i_1 is computed and with $R_2(\lambda)$ when i_2 is computed. The optical tracker output signals x_1 and x_2 are obtained as:

$$x_j(t) = g_j(t)^* i_j(t) \; j \in \{1,2\}, \qquad (9)$$

where t stands for kT, g_1 and g_2 are impulse responses of the selective amplifiers, and $*$ means temporal convolution. Based on (8) and (9) the following is obtained:

$$x_1(t) = g_{11}(t)^* s_1(t) + g_{12}(t)^* s_2(t)$$
$$+ g_{13}(t)^* [s_1(t) s_2(t)]$$
$$x_2(t) = g_{21}(t)^* s_1(t) + g_{22}(t)^* s_2(t)$$
$$+ g_{23}(t)^* [s_1(t) s_2(t)], \qquad (10)$$
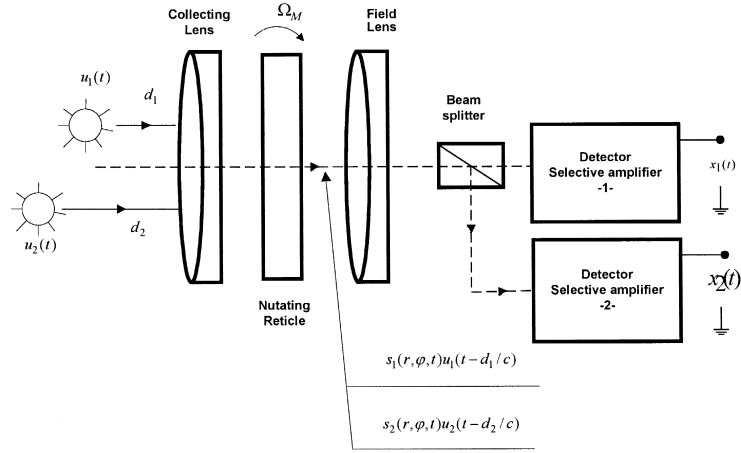
Fig. 3. The modified optical tracker.

where impulse responses g_{ij}, $i,j \in \{1,2,3\}$ can be identified from (8), (9) and (10) as:

$$g_{11}(t) = A_1 g_1(t) B_{11}(\lambda,t),$$

$$g_{12}(t) = A_1 g_1(t) B_{12}(\lambda,t),$$

$$g_{13}(t) = A_1 g_1(t) 2 K_1 K_2 \sqrt{B_{11}(\lambda,t) B_{12}(\lambda,t)}$$
$$\times \text{Re}\{\gamma_{12}(\Delta t)\}$$

$$g_{21}(t) = A_2 g_2(t) B_{21}(\lambda,t),$$

$$g_{22}(t) = A_2 g_2(t) B_{22}(\lambda,t),$$

$$g_{23}(t) = A_2 g_2(t) 2 K_1 K_2 \sqrt{B_{21}(\lambda,t) B_{22}(\lambda,t)}$$
$$\times \text{Re}\{\gamma_{12}(\Delta t)\}$$

$$B_{11}(\lambda,t) = \int \tau(\lambda) I_1(\lambda,t) R_1(\lambda) d\lambda$$

$$B_{12}(\lambda,t) = \int \tau(\lambda) I_2(\lambda,t) R_1(\lambda) d\lambda$$

$$B_{21}(\lambda,t) = \int \rho(\lambda) (I_1(\lambda,t) R_2(\lambda) d\lambda$$

$$B_{22}(\lambda,t) = \int \rho(\lambda) I_2(\lambda,t) R_2(\lambda) d\lambda \tag{11}$$

In relation to the signal model derived in [1] the model (10) is more complete. The linear model from [1] is obtained as a special case when incoherence between optical fields is assumed. If only the basic optical tracker construction is used (see Fig. 1) then Eq. (10) shows that optical tracker sees convolutive

combination of the two modulating functions s_1 and s_2. It has been shown analytically in [4] that in such a case the optical tracker follows the centroid the coordinates of which are functions of the effective brightness of the two sources. The point is that optical tracker fails to determine the accurate coordinates of either of the two sources. That is known as IR jamming problem. Although this problem, associated with the reticle based tracking systems, is very old there are still new attempts to design jamming resistant reticle seekers [30–32]. Basically these attempts assume that jammers can be detected on the basis of the energy and spectral discrimination. It is also assumed that, when jamming is detected, sensor signal is replaced with the predicted version based on the past values provided that target performs no maneuvering. These assumptions are partially true for the anti-aircraft missile scenario but generally do not hold in the anti-tank missile engagement [33]. A
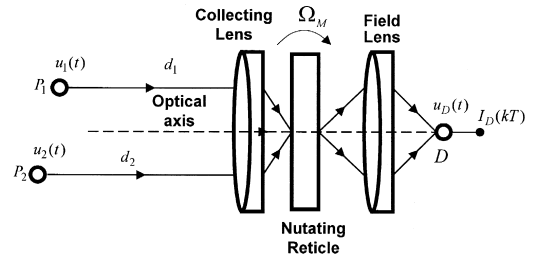
Fig. 4. Detection of optical radiation from two sources.
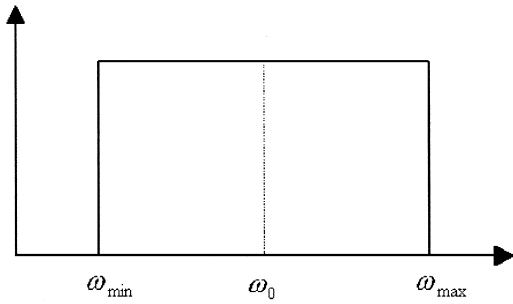
Fig. 5. Optical tracker band-pass region.

new approach was proposed in [1] and is extended here. It is based on the independent component analysis theory and an appropriate modification of the optical tracker design that for the case of two sources is shown on Fig. 3. Generally, ICA enables source signals s_1 and s_2, Eq. (10), to be recovered on the basis of the observed signals x_1 and x_2 only. Since the nonlinear ICA algorithms are designed for the special types of the non-linearity only, transformation of the non-linear convolutive model (10) into linear one would be of great importance. Let the optical tracking system is designed such that:

$$\omega_{min} > \frac{\omega_{max}}{2} \qquad (12)$$

where ω_{min} and ω_{max} are minimal and maximal corner frequencies of the optical tracker selective amplifiers, respectively, Fig. 5. When the source signals s_1 and s_2 are multiplied, two new parts of the frequency spectrum are generated that, in general, cause non-linear signal distortions. That can be avoided provided that the following inequalities are fulfilled:

$$\omega_{ij} + \omega_{ji} > \omega_{max} \qquad (13a)$$

$$|\omega_{ij} - \omega_{ji}| < \omega_{min} \qquad (13b)$$

where $\omega_{ij}, i,j \in \{1,2\}$ are corner frequencies of the source signals s_1 and s_2. It is easy to show that this can be fulfilled if the optical tracking system is designed such that (12) is ensured. Namely, the worst case for the inequality (13a) is occurred when $\omega_{ij} = \omega_{ji} = \omega_{min}$. Then (13a) is transformed into $\omega_{min} > (\omega_{max})/(2)$. For the inequality (13b) the worst case is occurred when $\omega_{ij} = \omega_{max}, \omega_{ji} = \omega_{min}$. Then

(13b) is transformed again into $\omega_{min} > (\omega_{max})/(2)$. Both conditions are obviously fulfilled when (12) is ensured. Then, the non-linear model (10) can be transformed into linear one by applying linear band-pass filtering operation on the measured signals x_1 and x_2 of the signal model (10). The new model is obtained:

$$\hat{x}_1(t) = \hat{g}_{11}(t)^* s_1(t) + \hat{g}_{12}(t)^* s_2(t)$$

$$\hat{x}_2(t) = \hat{g}_{21}(t)^* s_1(t) + \hat{g}_{22}(t)^* s_2(t) \qquad (14)$$

where $\hat{g}_{ij}(t) = h_{BP}(t)^* g_{ij}(t)$, $i,j \in \{1,2\}$ and h_{BP} is impulse response of the linear band-pass filter with the corner frequencies ω_{min} and ω_{max}.

4. Interpretation of the ICA theory requirements

Independent component analysis also known as blind source separation is a fundamental problem in signal processing. The problem is described for a number of source signals coming from different sources and a number of receivers [16]. Each receiver (antenna, microphone, photodiode,...) receives a linear combination of these source signals. Neither the structure of the linear combination nor the source signals are known to the receivers. In this environment the identification of the linear combinations is called the blind identification problem and the decoupling of the linear combinations is called the blind source separation problem [16]. In this paper we are considering the blind source separation problem. Two cases of linear mixture are possible: scalar and convolutive. Since, in our application measured signals are convolutive combination of the source signals (Eqs. (10), (11) and (14)) the convolu-
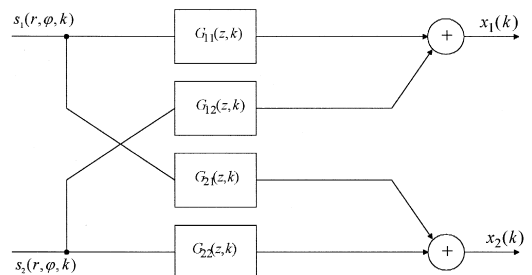
Fig. 6. Convolutive signal model.

Fig. 7. Feedback separation network.

Fig. 8. Power spectrum of the source signal s_1.
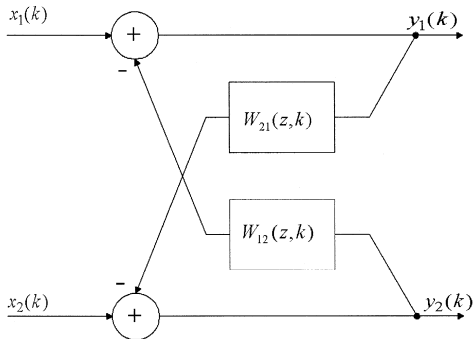
tive mixing case will be treated in this paper. Convolutive mixture is mathematically described by:

$$x = G^* s \qquad (15)$$

where G is the matrix of impulse responses. For decoupling the convolved signals (see (14) and Fig. 6) the feedback separation network shown in Fig. 7 will be used. A feedback separation network is preferred over a feed-forward network in order to avoid the whitening effect [22]. The decoupling filters $W_{12}(z)$ and $W_{21}(z)$ must be adjusted so that the transfer function $Q(z) = W(z) \times G(z)$ of the combined system will be of the form [17–19]:

$$Q(z) = \begin{bmatrix} Q_{11}(z) & 0 \\ 0 & Q_{22}(z) \end{bmatrix} \qquad (16)$$

or

$$Q(z) = \begin{bmatrix} 0 & Q_{12}(z) \\ Q_{21}(z) & 0 \end{bmatrix} \qquad (17)$$

In both these cases the source signals will be reconstructed up to the shaping filters $Q_{ij}(z)$. There are three fundamental assumptions on which all ICA algorithms are based: *statistical independence of the source signals, the source signals are non-Gaussian and the non-singularity of the mixing matrix in the model of the observed signals*. The question of whether these assumptions are fulfilled for the model of the modified optical tracker's output signals (given by (10) or (14)) are examined briefly at this point. The statistical independence assumption of the source signals $s_1(r,\varphi,t)$ and $s_2(r,\varphi,t)$ is reasonable since
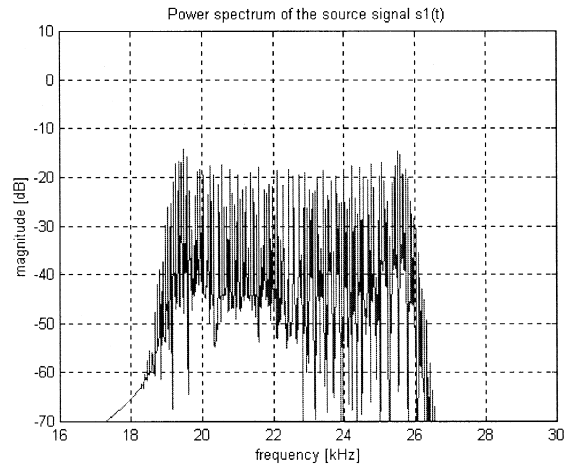
they are generated by two different (independent) optical sources. Figs. 8 and 9 show power spectrums of the two FM source signals. The absolute extreme values of the auto-correlation $C_2 s_1$, $C_2 s_2$ and cross-correlation $C_{11} s_1 s_2$ as well as of the fourth order cumulants $C_4 s_1$, $C_4 s_2$ and cross-cumulant $C_{22} s_1 s_2$ are given in Tables 1 and 2, respectively. It can be seen that in both cases the cross-statistics are approximately 10 times smaller than auto-statistics. Assuming statistical independence, the joint probability
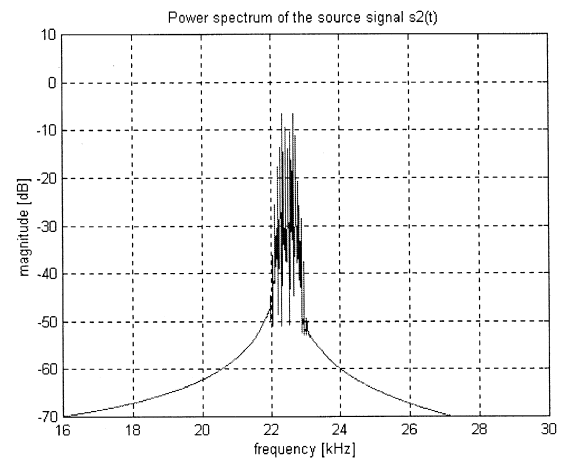
Fig. 9. Power spectrum of the source signal s_2.

Table 1
Second order statistics

Second order statistics	$C_2(S_1)$	$C_2(S_2)$	$C_{11}(S_1S_2)$
Maximal absolute value	0.5	0.5	0.068

density function (pdf) $f(s)$ of the vector of source signals is given as:

$$f(s) = \prod_{i=1}^{n} f_i(s_i) \tag{18}$$

where $f_i(s_i)$ is the marginal probability density function of the ith related component. The second assumption, that the source signals are non-Gaussian, for signals $s_1(r,\varphi,t)$ and $s_2(r,\varphi,t)$ is also fulfilled for the following reasons. It has been shown in (3) that the source signals are FM signals. These types of signals, as most communication signals, belong to the sub-Gaussian class of signals having negative kurtosis, where kurtosis of the signal x is defined as:

$$\kappa(x) = \frac{C_4 x}{C_2^2 x} \tag{19}$$

and C_{4x} is fourth order cumulant and C_{2x} is second order cumulant of the signal x. The kurtosis shows how far the signal is from the Gaussian distribution, which has kurtosis equal to zero. This is due to the fact that random processes with Gaussian distributions have all cumulants of order three or more equal to zero [34–36]. Fig. 10 shows estimated pdf of the source signal s_1 (Fig. 8). The shape of the pdf characteristic for the sub-Gaussian processes (tend to the uniform distribution) can be observed. The estimated value of the kurtosis is $\kappa(s_1) = -1.49$. When the previous two assumptions hold, all ICA algorithms recover the source signals by minimizing or maximizing certain criteria that indirectly factorizes the joint probability density function of the recovered signals. Since the source signals are independent by assumptions, the discussed factorization actually reconstructs the source signals. A consequence of such a separation criteria is that the separated

Table 2
Fourth order statistics

Fourth order statistics	$C_4(S_1)$	$C_4(S_2)$	$C_{22}(S_1S_2)$
Maximal absolute value	0.375	0.369	0.034
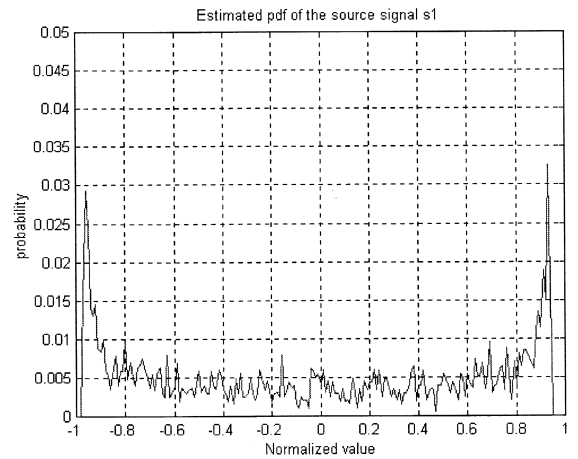
Fig. 10. Estimated pdf of the source signal s_1.

signals in principle represent scaled and permuted version of the source signals [16–18]. The third assumption is the non-singularity of the mixing matrix when the convolutive model (10) i.e. (14) is transformed into the frequency domain. We shall first assume that the optical sources u_1 and u_2 are incoherent. Since, $\gamma_{12}(\Delta t) = 0 \forall \Delta t$, g_{13} and g_{23} are zero (see Eq. (11)), signal model (10) is reduced to the linear convolutive model. It is experimentally shown in [1] that in such a case it is indeed possible to estimate the source signals s_1 and s_2 when only tracker output signals x_1 and x_2 are known. The non-singularity requirement means that measured signals x_1 and x_2 must be linearly independent combinations of the source signals s_1 and s_2, which ensures a benefit from using two sensors. It is shown in [1] that this assumptions holds. The signal model (10) transformed into the frequency domain yields:

$$\begin{bmatrix} X_1 \\ X_2 \end{bmatrix} = \begin{bmatrix} G_{11} & G_{12} \\ G_{21} & G_{22} \end{bmatrix} \times \begin{bmatrix} S_1 \\ S_2 \end{bmatrix} + \begin{bmatrix} G_{13} \\ G_{23} \end{bmatrix} \times (S_1S_2) \tag{20}$$

where all quantities in the Eq. (20) are Discrete Fourier Transforms (DFTs) of the related time domain quantities in the signal model (10). The frequency variable ω is dropped in Eq. (20) in order to simplify notation. When the optical fields are incoherent G_{13} and G_{23} are zero and nonsingularity condition is transformed into:

$$G_{11}G_{22} - G_{12}G_{21} \neq 0 \tag{21}$$

Inserting DFTs of the impulse responses (11) in (21) gives the following inequality:

$$\int \tau(\lambda) R_1(\lambda) I_1(\lambda,t) d\lambda \times \int R_2(\lambda) I_2(\lambda,t) d\lambda$$

$$- \int \tau(\lambda) R_1(\lambda) I_1(\lambda,t) d\lambda$$

$$\times \int \tau(\lambda) R_2(\lambda) I_2(\lambda,t) d\lambda$$

$$\neq \int \tau(\lambda) R_1(\lambda) I_2(\lambda,t) d\lambda \times \int R_2(\lambda) I_1(\lambda,t) d\lambda$$

$$- \int \tau(\lambda) R_1(\lambda) I_2(\lambda,t) d\lambda$$

$$\times \int \tau(\lambda) R_2(\lambda) I_1(\lambda,t) d\lambda, \qquad (22)$$

Provided that $R_1(\lambda) \cong R_2(\lambda) \cong R(\lambda)$ the inequality (22) is transformed in [1]:

$$\int \tau(\lambda) R(\lambda) I_1(\lambda,t) d\lambda \times \int R(\lambda) I_2(\lambda,t) d\lambda$$

$$\neq \int \tau(\lambda) R(\lambda) I_2(\lambda,t) d\lambda \times \int R(\lambda) I_1(\lambda,t) d\lambda$$
$$(23)$$

The inequality (23) is fulfilled when:

$$\tau(\lambda) \neq \text{const} \qquad (24)$$

over the wavelength region of interest that is fulfilled for real beam splitters [1]. Requirement (24) has quite general importance since in Eqs. (12)–(14) it has been shown that under proper condition of the optical tracker design the non-linear model (10), generated by the coherent optical sources, can be transformed into linear model (14) by simple linear band-pass filtering operations.

Nevertheless, we shall consider now the case when the optical sources are mutually coherent to a certain degree. That can occur when both points on Fig. 3 are illuminated from the same quasimonochromatic optical source (for example a single mode laser). Such situation is possible to happen in a case of guided missile systems which are using lasers for target designation (a common case in air to surface

missile systems). Optical signals u_1 and u_2 can be seen as both spatially shifted and temporally delayed. The mutual coherence function $\gamma_{12}(\Delta t)$ can be replaced with the selfcoherence function $\gamma(\Delta t)$. The value of $\gamma(\Delta t)$ depends on the relation between the relative delay Δt due to the path length difference and coherence time τ_c of the illuminating optical source. When single mode lasers are used as target designators the coherence time can have value of a few tents of nanoseconds giving the value for path length difference of 10 or 20 meters. Depending on the width of the laser beam it is probable that beside the target some other object be illuminated giving at the detector coherent optical radiation. What is important is that signal model (10) is nonlinear, which makes the problem of blind discrimination of the optical sources more difficult than in the incoherent case. Only a few papers deal with the nonlinear ICA [13,25–28]. Beside nonlinearity, which causes problems from the algorithmic point of view, a question that must be considered is whether the nonsigularity condition is fulfilled for the nonlinear model. We first examine this question on the linear parts of the signal model (10) and (11). If the linear parts of the measured signals x_1 and x_2 are linearly independent, then we will assume that the contribution from the nonlinear parts does not cause total information redundancy between x_1 and x_2. If we take into account that u_1 and u_2 are generated by the same source then:

$$I_1(\lambda,t) = c_1 I(\lambda,t), \; I_2(\lambda,t) = c_2 I(\lambda,t),$$

$$c_1, c_2 \in \Re, \qquad (25)$$

Inserting this in the inequality (22) yields:

$$\int I(\lambda,t) R_2(\lambda) d\lambda \neq \int I(\lambda,t) R_2(\lambda) d\lambda \qquad (26)$$

which obviously is not the truth. In the case of the coherent optical fields the nonsingularity of the linear part of the mixing matrix (20) cannot be ensured. In order to ensure that the measured signals x_1 and x_2 does not contain the same information the contribution from the nonlinear parts of the signal model (10) and (20) must not be equal. It means that impulse responses g_{13} and g_{23} must not be equal.

Taking into account Eq. (25) the DFTs of the impulse responses g_{13} and g_{23} yields:

$$G_{13}(\omega) = G_1(\omega) A_1 2 K_1 K_2 \sqrt{c_1 c_2}$$
$$\times \int \tau(\lambda) I(\lambda, t) R_1(\lambda) d\lambda \times \mathrm{Re}\{\gamma(\Delta t)\}$$

$$G_{23}(\omega)$$
$$= G_2(\omega) A_2 2 K_1 K_2 \sqrt{c_1 c_2} \int I(\lambda, t) R_2(\lambda) d\lambda$$
$$\times \mathrm{Re}\{\gamma(\Delta t)\} - G_2(\omega) A_2 2 K_1 K_2 \sqrt{c_1 c_2}$$
$$\times \int \tau(\lambda) I(\lambda, t) R_2(\lambda) d\lambda \times \mathrm{Re}\{\gamma(\Delta t)\}$$
$$(27)$$

Provided that $R_1(\lambda) \cong R_2(\lambda) \cong R(\lambda)$ and $G_1(\omega) \cong G_2(\omega) \cong G(\omega)$, $G_{13}(\omega)$ and $G_{23}(\omega)$ will not be equal if:

$$\tau(\lambda) \neq 0.5 \qquad (28)$$

which is the weaker condition compared with the condition (24) obtained for the case of incoherence. So the fulfilment of the condition (24) enables the applicability of the ICA theory to solve the multi-source limitation problem of the optical trackers for both coherent and incoherent optical sources. However, transformation of the nonlinear model (10) into linear (14) by performing linear band-pass filtering is preferable solution for the coherent optical sources.

5. The ICA algorithms

Ideally, the joint probability density function of the vector of the source signals is factorized when all cross-statistics between components of the signal vector are zero. Provided that non-Gaussian real scalar processes $s_1(r, \varphi, k)$ and $s_2(r, \varphi, k)$ have trispectra different from zero, that is:

$$S_{s_i s_i s_i s_i}(\omega_1, \omega_2, \omega_3) \neq 0$$
$$\forall \omega_1, \omega_2, \omega_3 i = 1,2$$

and cross-trispectra equal to zero, i.e.:

$$S_{s_i s_j s_k s_l}(\omega_1, \omega_2, \omega_3) = 0 \forall \omega_1, \omega_2, \omega_3$$
$$\forall i, j, k, l \in \{1,2\} \text{ except } i = j = k = l$$

it has been shown in [18] that the transfer function $Q(z)$ of the combined system will be diagonal when the following conditions are fulfilled:

$$S_{y_1 y_1 y_1 y_2}(\omega_1, \omega_2, \omega_3) = 0 \forall \omega_1, \omega_2, \omega_3$$
$$S_{y_2 y_2 y_2 y_1}(\omega_1, \omega_2, \omega_3) = 0 \forall \omega_1, \omega_2, \omega_3 \qquad (31)$$

Eq. (31) represents the criteria for signal separation in the frequency domain. The equivalent criteria in the time domain is given by:

$$\mathrm{cum}\left[y_1(k), y_1(k + \tau_1), y_1(k + \tau_2), y_2(k + \tau_3)\right]$$
$$= 0 \forall \tau_1, \tau_2, \tau_3$$
$$\mathrm{cum}\left[y_2(k), y_2(k + \tau_1), y_2(k + \tau_2), y_1(k + \tau_3)\right]$$
$$= 0 \forall \tau_1, \tau_2, \tau_3 \qquad (32)$$

The fourth order cross-cumulants in (32) are obtained as the Inverse Discrete Fourier Transform (IDFT) of the related cross-trispectra (40) [34,35]. This is equivalent to saying that the output signals will be separated when their mutual fourth-order statistics is zero [17,34]. Assuming that $W_{12}(z)$ and $W_{21}(z)$ are FIR filters of order M, the system of Eq. (32) is transformed in the system of at least $2M$ linear equations in terms of the filter coefficients w_{12} and w_{21} [17]. The solution is obtained by using an iterative algorithm that requires per iteration at least $2M^2 + 2M$ fourth-order sample cross-cumulants to be estimated. Due to the delay introduced by the block processing approach and the huge computational complexity of this approach such a solution is unacceptable for the real time separation of sources. The discrimination of the optical sources (Fig. 6) must be a real time process. Therefore, a real time version of the BSS algorithms is necessary. Such algorithms are given in [14,20–23] and are adaptive by nature. This means that at every time sample the algorithms should deliver instantaneous values of the separated signals $y_1(k)$ and $y_2(k)$. In [21] the adaptive separation is performed by minimizing the instantaneous energy of the separator output signals which actually decorrelates the signals and does not ensure statistical independence in the true sense. In [23] several approaches are given the most interesting of which are neural network separators based on the products of odd nonlinear activation functions and separators that minimize the squares of the fourth-order cross-cumulants such as given in (32). In [14,22] the separation of the convolved signals is achieved by maximizing the entropy of a sigmoid

function of the separator output signals. Here we present a class of adaptive blind separation algorithms for convolved sources which are based on the information maximization principle [14,22]. The input-output relations of the feedback network (Fig. 7) are given by:

$$y_1(k) = x_1(k) - \sum_{i=1}^{M} w_{12}(i) y_2(k-i)$$

$$y_2(k) = x_2(k) - \sum_{i=1}^{M} w_{21}(i) y_1(k-i) \qquad (33)$$

For causality reasons $w_{12}(0)$ and $w_{21}(0)$ must be zero. It is assumed that the source signals $s_1(r,\varphi,k)$ and $s_2(r,\varphi,k)$ have a zero mean and are statistically independent in the sense of (18). It has been shown in [14] that the maximization of the information transfer through the sigmoid function $z_1 = g(y_i)$ also reduces the redundancy between the outputs of the separation network y_i (Fig. 7). This process is also called independent component analysis that enables the network to solve the blind separation task. The mutual information between the sigmoid outputs and inputs is defined as [14]:

$$I(z,y) = H(z) - H(z/y) \qquad (34)$$

where $H(z)$ is the entropy of the sigmoid outputs, while $H(z/y)$ is the residual entropy in the output which did not come from the input. Since in the BSS scenario we have no noise (both signals and noise are treated equally) the entropy $H(z/y)$ has its lowest possible value: it diverges to $-\infty$ [14]. So the maximization of the mutual information $I(z/y)$ is equivalent to the maximization of the joint entropy $H(z)$ with respect to the separation filter coefficients:

$$\max_{w_{ij}} I(z,y) = \max_{w_{ij}} H(z) \qquad (35)$$

To see why the maximization of $H(z)$ separates signals y_i (i.e. factorizes joint probability density function $f(y)$) the mutual information (i.e. statistical independence between the components z_i) is expressed in a form of Kullback divergence [24]:

$$MI(z) = \delta\left(f(z), \prod_{i=1}^{n} f_i(z_i) \right)$$

$$= \int_{-\infty}^{\infty} f(z) \log \frac{f(z)}{\prod_{i=1}^{n} f_i(z_i)} dz \qquad (36)$$

$MI(z)$ vanishes if the components z_i are statistically independent and it is strictly positive otherwise [24]. Based on (36) the mutual information $MI(z)$ can be defined in terms of joint and marginal entropy $H(z)$ and $H(z_i)$ respectively:

$$MI(z) = -H(z) + \sum_{i=1}^{n} H(z_i) \qquad (37)$$

where the entropy terms are defined by [14]:

$$H(z) = -E[\log f(z)] = -\int_{-\infty}^{\infty} f(z)\log f(z)\, dz$$

$$H(z_i) = -E[\log f(z_i)] = -\int_{-\infty}^{\infty} f(z)\log f_i(z_i)\, dz \qquad (38)$$

It follows from (37) that:

$$H(z) = \sum_{i=1}^{n} H(z_i) - MI(z) \qquad (39)$$

It can be seen from (39) that the maximization of the joint entropy $H(z)$ actually maximizes the marginal entropy $H(z_i)$ and minimizes mutual information $MI(z)$ which, due to (36), leads to the factorization of $f(z)$. Since the z_i's are related to y_i's with some invertible transformation, as for example $z_i = \tanh(y_i)$, factorization of $f(z)$ will have as a direct consequence the factorization of $f(y)$. When $z = g(Wx)$ has a unique inverse, the multivariate probability density function can be written as [14]:

$$f(z) = \frac{f(x)}{|J|} \qquad (40)$$

where $|J|$ is the absolute value of the Jacobian of the transformation. The Jacobian is defined as the determinant of the matrix of partial derivatives:

$$J = \det \begin{bmatrix} \dfrac{\partial z_1}{\partial x_1} & \cdots & \dfrac{\partial z_1}{\partial x_n} \\ . & . & \\ \dfrac{\partial z_n}{\partial x_1} & \cdots & \dfrac{\partial z_n}{\partial x_n} \end{bmatrix} \qquad (41)$$

Then using (38) and (40) the joint entropy can be written as:

$$H(z) = -E[\ln f(z)] = E[\ln|J|] - E[\ln f(x)] \qquad (42)$$

Fig. 11. Power spectrum of the measured signal x_1.
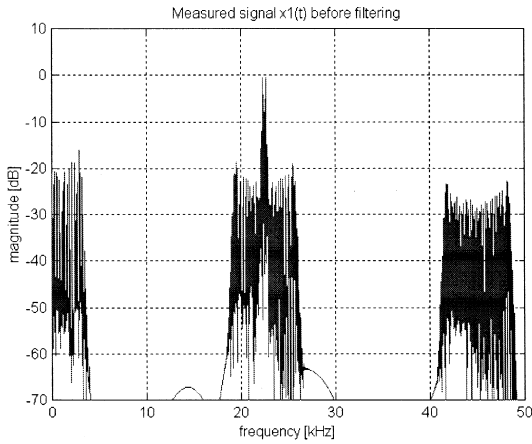
Fig. 12. Power spectrum of the filtered measured signal x_1.

Now, the maximization of $H(z)$ with respect to the coefficients of the separation filters w_{ij} is equivalent to the maximization of $\ln|J|$ since in Eq. (42) $\ln f(x)$ does not depend on w_{ij}. Hence,

$$\max_{w_{ij}} H(z) = \max_{w_{ij}} \ln|J| \qquad (43)$$

For the feedback separation network shown in Fig. 7. and described with the input-output relation (33) the absolute value of the Jacobian is obtained as:

$$|J| = \left|\det\left[\frac{\partial z_i}{\partial x_i}\right]_{ij}\right| = \left|\frac{\partial z_1}{\partial y_1} \cdot \frac{\partial z_2}{\partial y_2}\right| \qquad (44)$$

The adjustments of the separation filter coefficients are then obtained as:

$$\Delta w_{ij}(k,m) = \frac{\partial H(z)}{\partial w_{ij}(k,m)} = \frac{\partial \ln|J|}{\partial w_{ij}(k,m)}$$

$$= \frac{\partial}{\partial w_{ij}(k,m)} \ln \frac{\partial z_i}{\partial y_i}$$

$$\Delta w_{ij}(k,m) = \left(\frac{\partial z_i}{\partial y_i}\right)^{-1} \frac{\partial}{\partial w_{ij}(k,m)}\left(\frac{\partial z_i}{\partial y_i}\right) \qquad (45)$$

where k is the discrete time index, and m is the coefficient index of the related separation filter. If z_i is taken to be $\tanh(y_i)$ then $\partial z_i/\partial y_i = 1 - z_i^2$ and Eq. (45) becomes:

$$\Delta w_{ij}(k,m) = 2 z_i(k) y_j(k - m)$$

$$= 2\tanh(y_i(k)) y_j(k - m) \qquad (46)$$

From this the separator learning rule is obtained as:

$$w_{ij}(k + 1,m) = w_{ij}(k,m) + \mu \Delta w_{ij}(k,m)$$

$$= w_{ij}(k,m) 2\mu \tanh(y_i) y_j(k - m) \qquad (47)$$

where μ in Eq. (47) is a small positive constant also called the adaptation gain.

6. Simulation results

Measured signals x_1 and x_2 were generated according to the nonlinear signal model (10) on the basis of the two FM source signals s_1 and s_2 the power spectrums of which are shown on Figs. 8 and
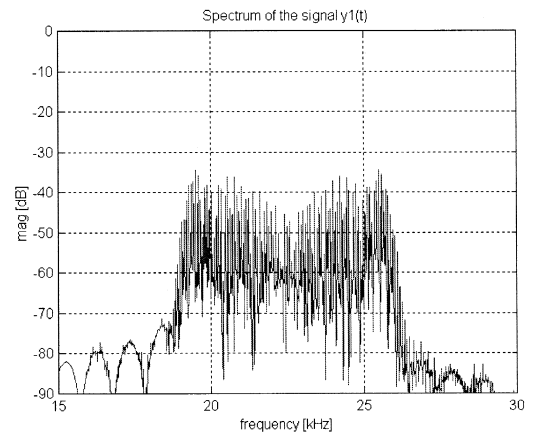
Fig. 13. Power spectrum of the reconstructed signal y_1.
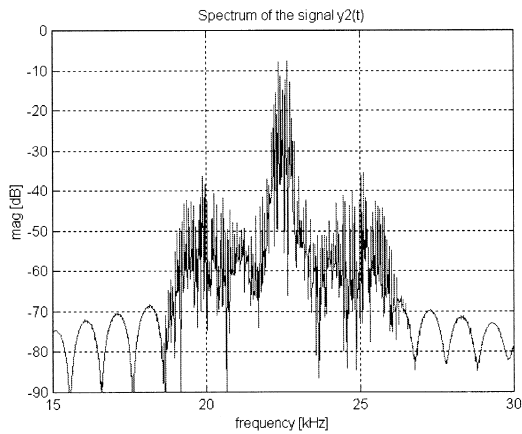
Fig. 14. Power spectrum of the reconstructed signal y_2.

9. The total coherence case, $\gamma_{12}(\Delta t) = 1$, was assumed. Power spectrum of the measured signal x_1 is shown on Fig. 11. The nonlinear effect due to the nonlinear part in the signal model (10) can be observed. Power spectrum of the measured signal x_2 looks very similarly. When, in accordance with the exposed analysis Eqs. (12)–(14), the linear bandpass filtering is applied on the measured signals x_1 and x_2, signals $\hat{x}_1$ and $\hat{x}_2$ are obtained, Eq. (14). Power spectrum of the signal $\hat{x}_1$ is shown on Fig. 12. It is obvious that nonlinear effect has been eliminated. Power spectrum of the signal $\hat{x}_2$ looks very similarly. When FM demodulator is applied on either signal $\hat{x}_1$ or signal $\hat{x}_2$, only the IR optical source that was placed near the center of the field of view (FOV) can be discriminated. If, however, the entropy based ICA algorithm, Eq. (47), is applied on the signals $\hat{x}_1$ and $\hat{x}_2$ the influence of the IR source placed near the center of the FOV can be eliminated and both IR sources can be discriminated. Power spectrums of the signals y_1 and y_2, according to Eq. (33), are shown on Figs. 13 and 14. It can be observed in signal y_1 that influence of the IR source placed near the center of the FOV is eliminated. Signal y_1 represents reconstructed version of the source signal s_1 while y_2 represents reconstructed version of the source signal s_2.

7. Conclusion

A statistical optics based analysis is performed that yields a mathematical model of the output sig-

nals of a modified optical tracker based on the rising-sun nutating reticle. It has been shown that coherence between optical sources produces a non-linear signal model that becomes linear when optical sources are incoherent. It has been also shown that for both coherent and incoherent optical sources, the nonsingularity of the mixing matrix in the frequency domain can be ensured requiring that the beam splitter transmission coefficient be non-constant over the wavelength region of interest. Thus the requirements necessary for the ICA theory to work are fulfilled for both coherent and incoherent optical sources. However, it has been additionally shown that by the proper design of the optical tracker the nonlinear model, generated by the coherent optical sources, can be converted into linear one by simple linear bandpass filtering operation. Consequently, the multisource limitation of the nutating rising-sun reticle based optical trackers can in principle be overcome for both coherent and incoherent optical sources.

References

[1] I. Kopriva, A. Peršin, Discrimination of optical sources by use of adaptive blind source separation theory, Appl. Opt. 38 (1999) 1115–1126.

[2] R.D. Hudson, Jr., Optical modulation, Infrared System Engineering, Chap. 6, Wiley, New York, 1969, pp. 235-263.

[3] G.F. Aroyan, The technique of spatial filtering, Proc. Inst. Radio Engrs. 47 (1959) 1561–1568.

[4] A.F. Nicholson, Error signals and discrimination in optical trackers that see several sources, Proc. IEEE 53 (1965) 56–71.

[5] R.L. Driggers, C.E. Halford, G.D. Boreman, D. Lattman, K.F. Wiliams, Parameters of spinning FM reticles, Appl. Opt. 30 (7) (1991) 887–895.

[6] R.L. Driggers, C.E. Halford, G.D. Boreman, Parameters of spinning AM reticles, Appl. Opt. 30 (19) (1991) 2675–2684.

[7] K. Suzuki, Analysis of rising-sun reticle, Opt. Eng. 18 (3) (1979) 350–351.

[8] Z.W. Chao, J.L. Chu, General analysis of frequency-modulated reticles, Opt. Eng. 27 (6) (1988) 440–442.

[9] Z.W. Chao, J.L. Chu, Parameter analysis of frequency-modulation reticle design, Opt. Eng. 27 (6) (1988) 443–451.

[10] R.G. Driggers, C.E. Halford, G.D. Boreman, Marriage of frequency modulation reticles to focal plane arrays, Opt. Eng. 30 (10) (1991) 1516–1521.

[11] J.W. Goodman, Coherence of optical waves, Statistical Optics, Chap. 5, John Wiley, 1985, pp. 157-236.

[12] M.V. Klein, T.E. Furtak, Coherence, Optics, Chap. 8, John Wiley, 1986, pp. 507–582.

[13] T.W. Lee, Blind separation of time-delayed and convolved sources and First steps toward nonlinear ICA, Independent Component Analysis — Theory and Applications, Chap. 4, Kluwer AP, Boston, 1998, pp. 83–107; Chap. 6, pp. 123–137.

[14] A.J. Bell, T.J. Sejnowski, An information-maximization approach to blind separation and blind deconvolution, Neural Computation 7 (1995) 1129–1159.

[15] H.H. Szu, Progress in Unsupervised Learning and Real World Applications, Russian Academy of Nonlinear Sciences, 1999.

[16] X.R. Cao, R.W. Liu, General approach to blind source separation, IEEE Trans. Signal Processing 44 (1996) 562–571.

[17] D. Yellin, E. Weinstein, Criteria for multichannel signal separation, IEEE Trans. Signal Processing 42 (1994) 2158–2168.

[18] D. Yellin, E. Weinstein, Multichannel signal separation: methods and analysis, IEEE Trans. Signal Processing 44 (1996) 106–118.

[19] J. Wang, H. Zhenya, Blind identification and separation of convolutively mixed independent sources, IEEE Trans. Aerospace and Electron. Syst. 33 (1997) 997–1002.

[20] E. Weinstein, A.V. Oppenheim, M. Feder, J.R. Buck, Iterative and sequential algorithms for multisensor signal enhancement, IEEE Trans. Signal Processing 42 (1994) 846–859.

[21] S. Van Gerven, D. Van Compernolle, Signal separation by symmetric adaptive decorrelation: stability, convergence, and uniqueness, IEEE Trans. Signal Processing 43 (1995) 1602–1612.

[22] K. Torkkola, Blind separation of convolved sources based on information maximization, IEEE Workshop on Neural Networks for Signal Processing, Kyoto, Japan, September 4–6, 1996.

[23] H.L. Nguyen Thi, C. Jutten, Blind source separation for convolutive mixtures, Signal Processing 45 (1995) 209–229.

[24] P. Common, Independent component analysis, a new concept?, Signal Processing 36 (1994) 287–314.

[25] L. Molgedy, H.G. Schuster, Separation of a mixture of independent signals using time delayed correlations, Phys. Rev. Lett. 72 (1994) 3634–3637.

[26] H.H. Yang, S. Amari, A. Cihocki, Information-theoretic approach to blind separation of sources in non-linear mixture, Signal Processing 64 (1998) 291–300.

[27] T.W. Lee, B.U. Koehler, Blind source separation of nonlinear mixing models, IEEE International Workshop on Neural Networks for Signal Processing, Florida, September, 1997 (Institute for Electrical and Electronic Engineers, New York, 1997).

[28] A. Taleb, C. Jutten, S. Olympieff, Source separation in post nonlinear mixtures: an entropy based algorithm, International Conference Acoustics, Speech, Signal Processing, Seattle, Washington, May, 1998 (Institute for Electrical and Electronic Engineers, New York, 1998).

[29] H. Taub, D.L. Schilling, Frequency-modulation systems, Principles of Communication Systems, Chap. 4, McGraw-Hill, 1987, pp. 142–182.

[30] H.K. Hong, S.H. Han, J.S. Choi, Simulation of an improved reticle seeker using segmented focal plane array, Opt. Eng. 36 (3) (1997) 883–888.

[31] H.K. Hong, S.H. Han, J.S. Choi, Dynamic simulation of infrared reticle seekers and an efficient counter-countermeasure algorithm, Opt. Eng. 36 (8) (1997) 2341–2345.

[32] H.K. Hong, S.H. Han, J.S. Choi, Simulation of the spinning concentric annular ring reticle seeker and an efficient counter-countermeasure, Opt. Eng. 36 (11) (1997) 3206–3211.

[33] K. Ćosić, I. Kopriva, T. Kostić, M. Slamić, M. Volarević, Design and implementation of a hardware-in-the-loop simulator for semi-automatic guided missile system, Simulation Prac. Theor. 7 (3) (1999) 107–123.

[34] D.R. Brillinger, Foundations, Time Series Data Analysis and Theory, Chap. 2, McGraw-Hill, 1981, pp. 16–44.

[35] J.M. Mendel, Tutorial on higher-order statistics (Spectra) in signal processing and system theory: theoretical results and some applications, Proc. IEEE 79 (1991) 278–305.

[36] P. McCullagh, Elementary theory of cumulants, Tensor Methods in Statistics, Chap. 2, Chapman and Hall, 1987, 1995, pp. 24–46.